Available online at www.sciencedirect.com
SCIENCE DIRECT®
Bioorganic & Medicinal Chemistry 13 (2005) 2431–2438
Bioorganic & Medicinal Chemistry

Evaluation of macrocyclic Grb2 SH2 domain-binding peptide mimetics prepared by ring-closing metathesis of C-terminal allylglycines with an N-terminal β-vinyl-substituted phosphotyrosyl mimetic

Shinya Oishi,[a] Rajeshri G. Karki,[a] Zhen-Dan Shi,[a] Karen M. Worthy,[b] Lakshman Bindu,[b] Oleg Chertov,[b] Dominic Esposito,[c] Peter Frank,[c] William K. Gillette,[c] Melissa Maderia,[a] James Hartley,[c] Marc C. Nicklaus,[a] Joseph J. Barchi, Jr.,[a] Robert J. Fisher[b] and Terrence R. Burke, Jr.[a,*]

[a]*Laboratory of Medicinal Chemistry, Center for Cancer Research, National Cancer Institute, National Institutes of Health, PO Box B, Bldg. 376 Boyles St. Frederick, MD 21702-1201, USA*
[b]*Protein Chemistry, SAIC-Frederick, Frederick, MD 21702, USA*
[c]*Protein Expression Laboratory, SAIC-Frederick, Frederick, MD 21702, USA*

Received 8 December 2004; accepted 24 January 2005

Abstract—Preferential binding of ligands to Grb2 SH2 domains in β-bend conformations has made peptide cyclization a logical means of effecting affinity enhancement. This is based on the concept that constraint of open-chain sequences to bend geometries may reduce entropy penalties of binding. The current study extends this approach by undertaking ring-closing metathesis (RCM) macrocyclization between i and i + 3 residues through a process involving allylglycines and β-vinyl-functionalized residues. Ring closure in this fashion results in minimal macrocyclic tetrapeptide mimetics. The predominant effects of such macrocyclization on Grb2 SH2 domain binding affinity were increases in rates of association (from 7- to 16-fold) relative to an open-chain congener, while decreases in dissociation rates were less pronounced (approximately 2-fold). The significant increases in association rates were consistent with pre-ordering of solution conformations to near those required for binding. Data from NMR experiments and molecular modeling simulations were used to interpret the binding results. An understanding of the conformational consequences of such i to i + 3 ring closure may facilitate its application to other systems where bend geometries are desired.

The growth factor receptor bound 2 protein (Grb2)[1,2] provides important components of signaling associated with breast cancer.[3,4] Accordingly, functional inhibitors of Grb2 SH2 domain signaling have been pursued as leads to new anticancer therapeutics.[5,6] The development of Grb2 SH2 domain-binding antagonists has been guided by the preferential recognition of phosphotyrosyl (pTyr)-containing peptide sequences of the type 'pTyr-Xxx-Asn-Yyy', where the pTyr phenylphosphate group, the Asn side chain and lipophilic residues C-proximal to the Asn residue serve as important interaction determinants.[7] Structure **1** (Fig. 1) shows a hypothetical peptide based on this motif wherein Yyy is an amidoglycine residue. Because binding of ligands to Grb2 SH2 domains occurs in β-bend conformations,[8] macrocyclization has been used as an approach to enhance affinity, based on the concept that constraint of open-chain sequences to bend geometries may reduce entropy penalties of binding.[9,10] Ring-closing metathesis (RCM) has shown utility for peptide macrocyclization in a variety of contexts. The terminal alkene groups required for RCM ring closure can be introduced by several methods, including the insertion of allylglycine residues at the intended sites of ring juncture.[11] For peptide **1**, RCM macrocyclization between the i (pY) and i + 3 (Yyy) positions of the β-bend using this approach would yield

Keywords: Macrocycle; Grb2 SH2 domain; Peptide mimetic; Ring-closing metathesis.
* Corresponding author. Tel.: +1 301 846 5906; fax: +1 301 846 6033; e-mail: tburke@helix.nih.gov

0968-0896/$ - see front matter © 2005 Elsevier Ltd. All rights reserved.
doi:10.1016/j.bmc.2005.01.052

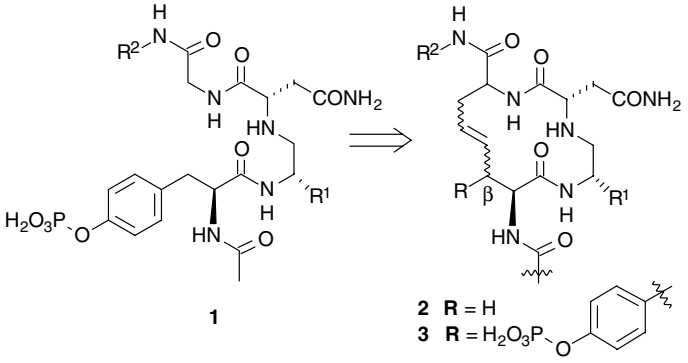

Figure 1. Structures of hypothetical open-chain and macrocyclized Grb2 SH2 domain-binding peptides.

structures of type **2** that lack critical phenylphosphate functionality needed for high affinity binding. However, by appending a phenylphosphate mimicking group onto the allylglycine β-position, macrocyclization with full retention of cognate functionality could be achieved (structure **3**).

This approach has recently been reported in modified form using a C-terminal i + 3 naphthylpropylamine unit that does not contain the α-carboxyl group of a true allylglycine residue (compounds **4**, Fig. 2).[12,13] The lack of an α-carboxyl group in compounds of type **4** significantly impedes C-terminal variation, since each new target macrocycle requires an individual total synthesis that begins with a lengthy preparation of the C-terminal 2-allyl-3-aryl-1-propanamido portion.[14,15] To circumvent these limitations, macrocycles **5** and **6** were designed as full embodiments of the general structure **3** that are based on the open-chain analogue **7**. Preparation of compounds **5** and **6** was achieved using commercially-available (1-naphthyl)methylamine and L- and D-allylglycines, respectively.[16] Both **5** and **6** employ RCM macrocyclization differently than previously reported accounts.[11,17–20] A potential advantage of this new approach not shared by earlier protocols that lead to macrocycles of type **4**, could be facile C-terminal variation through the use of readily available starting materials. The current report examines structural aspects of ligands derived from this type of macrocyclization and their relationship to Grb2 SH2 domain binding.

1. Results and discussion

1.1. Grb2 SH2 domain-binding affinity

Macrocycles **5** and **6** represent the first β-bend mimetics formed by i to i + 3 RCM ring closure of an allylglycine residue onto a β-functionalized residue.[16] To examine the potential value of this type of ring closure within a Grb2 SH2 domain-binding system, the affinities of **5** and **6** were compared with open-chain **7** using surface plasmon resonance (SPR) assays. Relative to open chain **7**, macrocycles **5** and **6** exhibited affinity enhancements of 32-fold and 12-fold, respectively (Table 1). The K_D values presented in Table 1 were calculated from association and dissociation rate constants (K_a and K_d, respectively). The potency enhancements based on kinetically-

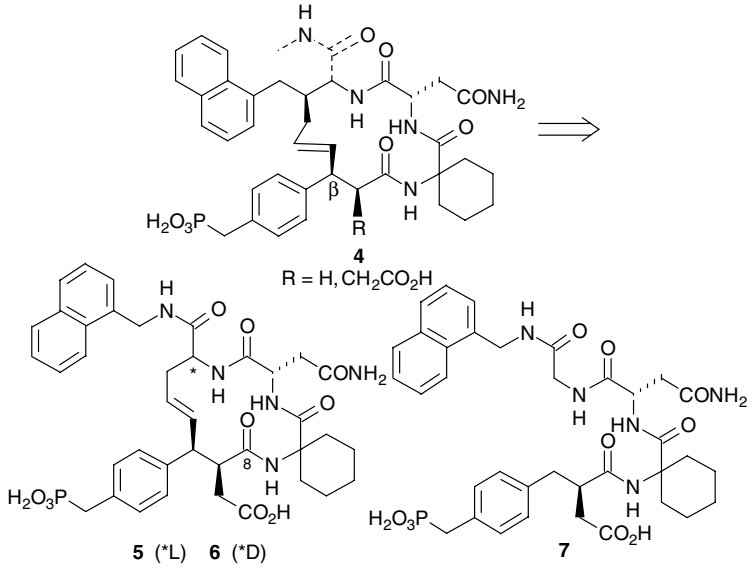

Figure 2. Structures of key compounds **5**–**7** and previously-reported macrocycles **4**.[12,13]

Table 1. Plasmon resonance-determined kinetic data for the binding to Grb2 SH2 domain protein[a]

No	K_a ($M^{-1}s^{-1}$)	K_d (s^{-1})	K_D (nM)	n
5	$3.58 \times 10^6 \pm 7.00 \times 10^3$	$6.75 \times 10^{-2} \pm 7.89 \times 10^{-5}$	18.8	3
6	$1.66 \times 10^6 \pm 1.40 \times 10^4$	$8.41 \times 10^{-2} \pm 3.28 \times 10^{-4}$	50.7	4
7	$2.23 \times 10^5 \pm 9.2 \times 10^3$	$1.33 \times 10^{-1} \pm 2.38 \times 10^{-2}$	599	2

[a] Data was obtained as described in the Experimental section.

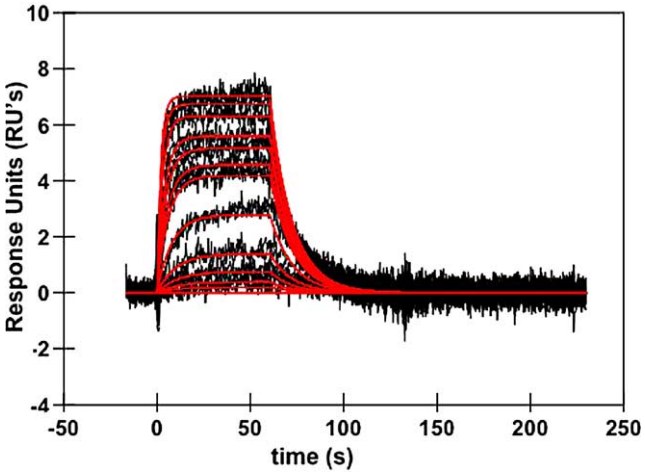

Figure 3. Example of SPR data (black) and data fit (red) for interaction of **6** with chip-bound Grb2 SH2 domain protein.

determined K_D values, are less than those calculated using steady-state K_D values.[16] The reasons for this are not known. A representative SPR data plot with its associated data fit are shown in Figure 3. The predominant effects on binding affinity incurred by macrocyclization are increases in rates of association relative to open-chain **7** (16-fold for **5** and 7-fold for **6**), while decreases in dissociation rates relative to **7** are less pronounced (2-fold for **5** and 1.6-fold for **6**). The significant increases in association rates are consistent with pre-ordering of solution conformations to approximate those required for binding. However, this is in contrast to a recent study that found no increase in Grb2 SH2 domain-binding affinity following RCM macrocyclization, even though modeling studies showed that ring-closed conformations were similar to those observed in the X-ray structure of a Grb2 SH2 domain-bound linear peptide.[20] These latter results indicate that constraining solution conformations to those found in the bound peptide do not necessarily enhance overall affinity. Similar results have been observed in other SH2 domain-binding systems,[21,22] where a phenomenon of enthalpy–entropy compensation has been invoked.[23] NMR and molecular modeling studies were undertaken to examine the effects of macrocyclization on conformation and their potential relationships to interactions with the Grb2 SH2 domain.

1.2. NMR studies

Since the hypothesis behind macrocyclization as an approach toward affinity enhancement is a pre-ordering of the inhibitors to bend geometries needed for binding, it was of interest to determine and compare the preferred conformations of the open chain and macrocyclic compounds in solution. Therefore, a battery of NMR experiments was performed to ascertain whether specific dispositions around the macrocycle were evident. For standard β-turns in natural peptides, there are sets of distinct coupling constants and NOE patterns that are typically observed.[24] In the case of compounds **5** and **6**, these patterns would be different due to the number of linker atoms employed for macrocyclization, the inflexibility of the olefin moiety included in the linkers and constraining effects of the β-bend-inducing cyclohexyl residue. The use of 3-carbon linkers dramatically restricts the available conformational space of the macrocycle as shown by both NMR data and molecular modeling (vide infra).

All molecules examined were assigned by standard techniques (COSY, TOCSY, NOESY, ROESY) by collecting NMR data in D_2O, 90% H_2O/D_2O, and DMSO-d_6 to allow assignment and evaluation of the solution behavior of the exchangeable protons. Both NOESY and ROESY spectra showed only a sparse set of NOE's, with the majority being sequential or short range in nature. This data offered little in the way of structural restraints. Nevertheless, the observed NOE's were qualitatively grouped (strong, medium, weak) and used as filtering criteria to choose 'best fit' structures after exhaustive in silico conformational searching (see the Modeling Section). Additional NMR experiments were conducted to explore the shielding or hydrogen-bonding characteristics of the three endocyclic and one exocyclic amide groups. Temperature coefficients were examined in DMSO-d_6 for compounds **5**, **6**, and **7** (Fig. 4). Chemical shift changes plotted against temperature gave linear relationships indicating that conformational changes were minimal over the temperature range (20–55 °C, Fig. 4B). Values for $\Delta\delta$/°C ranged from 0 to −5.54 ppb/°C (Fig. 4C), suggesting that there is considerable shielding of certain protons. Specifically, NH^2 and NH^3 (numbering as in Fig. 4A) showed the lowest negative values for all three compounds. This was consistent with solvent shielding or their involvement in intramolecular hydrogen bonds. The lowest values were seen for NH^2, which is the amide proton that would be involved in a typical β-turn (i to i + 3)-type hydrogen-bond. However, it is unlikely that this amide proton extends across the macrocycle ring to hydrogen bond with the carbonyl at C8 (see numbering in Fig. 2). Interestingly, distinct chemical shifts were observed for each of the Asn side chain amide protons, and their temperature coefficients were fairly low (−3 to −4.8 ppb/°C). This suggested that an extended hydrogen bonding network may exist with neighboring donor acceptor pairs around the macrocycle.

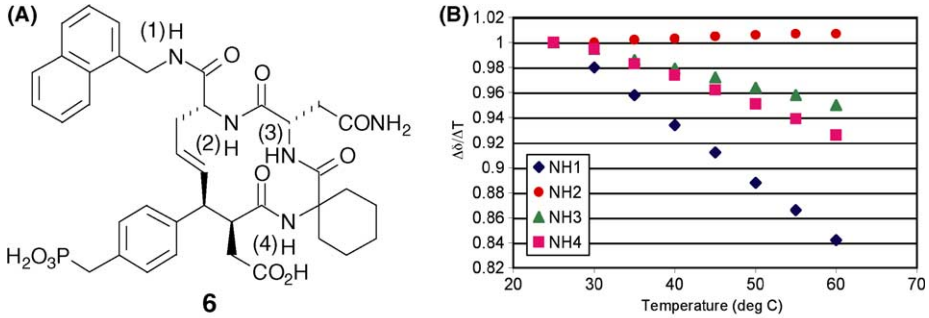

(C)

	Δδ/ΔT (ppb/ C)		
Amide Proton	**5**	**6**	**7**
NH1	-4.5	-3.7	-2.5
NH2	0.2	-1.0	-2.4
NH3	-1.4	-3.5	-3.0
NH4	-2.1	-4.0	-5.5

Figure 4. Temperature coefficients for the four amide protons of compounds **5**, **6**, and **7** measured in DMSO-d_6. (A) Labeling of amide protons as shown for compound **6**. (B) Representative graph of values for **5** showing the linearity of the fits. (C) Table of coefficient values in parts per billion per degree C.

An attempt was made to corroborate these data by calculating H/D exchange rates for four of the amide protons. Data was collected for compounds **5** and **7**, with compound **6** not being analyzed due to limited solubility of its free acid in D_2O. Although both **5** and **7** showed rapid exchange of all amides after dissolution in D_2O, it was possible to show that for **5**, the slowest exchange was observed for NH^3, followed by NH^4, NH^2, and NH^1. For the open chain **7**, the slowest exchange was observed for NH^2, suggesting that this amide has more freedom to participate in cross-ring hydrogen bonding that would define a typical β-turn. It is interesting to note that although **7** has the ability to extend its carbon backbone, the data strongly suggests that the molecule remains at least partially folded in solution.

1.3. Molecular modeling studies

Since the relative paucity of NMR information precluded prediction of specific structural elements, a comprehensive modeling study was performed on **5**, **6**, and **7** to explore the extent of conformational space available to the molecules. In particular, it was of interest to examine the various rotamer populations allowed for the two exocyclic aromatic residues, since NMR did little to define the positions of these moieties. Accordingly, hypothetical binding modes of these molecules were derived from molecular dynamics simulations followed by further analysis of each of the minimized protein–ligand complexes.

In the lowest energy complexes, the i + 2 Asn residues in **5**, **6**, and **7** made hydrogen bonding interactions with the carbonyl of LβE4[25] (L120) and bidentate hydrogen bonding interactions with the backbone carbonyl and amide protons of LysβD6 (K109), respectively (Fig. 5). The backbone amide of the pY + 1 aminocyclohexanecarboxylic acid (Ac_6c) residue was hydrogen bonded to the carbonyl group of HβD4 (H107), while the pTyr mimetic phosphonate group interacted with SBC2 (S90) and RβB5 (R86) residues. For peptides **5** and **6**, interaction with RαA2 (R67) is mediated by the α-CH_2COOH, while this interaction is absent in peptide **7**. Hydrogen bonding with the RαA2 residue is a characteristic of Grb2 SH2 domain inhibitors that is normally mediated by the pTyr phosphate (or phosphonate) group. The absence of such an interaction with RαA2 in case of **7** could reduce its binding affinity. However, interactions between the phosphonate groups of **5** and **6** and the RαA2 residue also appear to be missing in spite of the

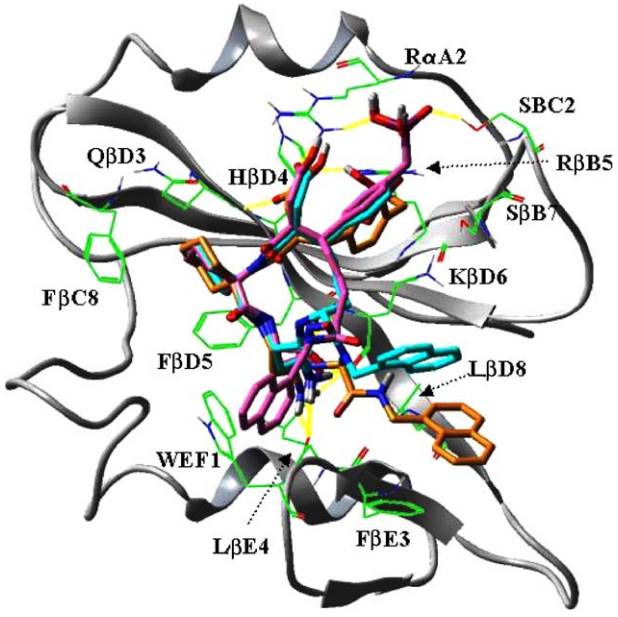

Figure 5. Hypothetical Grb2 SH2 domain binding modes of **5**–**7**. Hydrogen bonds are represented as dotted lines in yellow. For reasons of clarity, only key residues and atoms are shown. Color codes used: nitrogen—blue; oxygen—red; phosphorus—maroon; hydrogen—gray; carbon atoms—pink (for **5**); cyan (for **6**); and orange (for **7**).

fact that these peptides exhibit high binding affinity. The loss of phosphonate interactions with the RαA2 residue may be due to conformations arising from the size of the macrocyclic ring, which is one unit shorter than previously reported high affinity macrocyclic Grb2 SH2 domain binding inhibitors.[13] The most notable difference observed between **5** and **6** appears to be the absence of hydrophobic interactions between the C-terminal naphthyl amide moiety of **5** and residues LβD8 (L111) and KβD6 (K109).

Based on binding orientations in the lowest energy complexes, one would expect peptide **5** to exhibit less affinity than peptide **6**. The fact that this is contrary to observation may indicate understanding affinity differences cannot be done merely on the basis of lowest energy complexes. In light of this, the conformational space of the ligands was explored in both the free and the bound states. To perform these studies, peptides **5**, **6**, and **7** were extracted from their complexed states and subjected to 5000 steps of Monte Carlo Multiple Minimum (MCMM)[26] using Merck Molecular Force Field (MMFFs)[27] with a continuum H_2O solvation model (GB/SA).[28] Conformers within 50 kcal/mol of the global energy minimum were stored and subjected to cluster analysis using XCluster (Schrödinger Inc.).[29] For each compound, average conformations of molecules that were parts of clusters with high separation ratios were saved and the inter-proton distances were measured. These inter-proton distances were than compared with NMR NOESY-derived inter-proton distances in order to arrive at the closest solution conformer for each of **5**, **6**, and **7**, respectively.

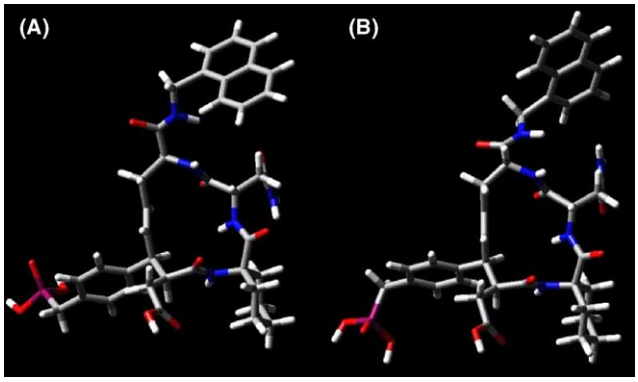

Figure 6. Average solution conformer of **5** (A) and **6** (B) derived using a combination of modeling and NMR results.

It was possible to identify a select subset of conformers for macrocycles **5** and **6** that were consistent with the results of NMR solution studies. However, because of the greater flexibility of **7**, clusters of conformers could not be obtained with high separation ratios, even though NMR data suggested that **7** remained at least partially folded in solution. Attempts to pre-screen the generated conformers of **7** using NMR-derived distance constraints, followed by cluster analysis, also failed to provide good clustering. This implied that **7** can fold itself in multiple ways, owing to its greater conformational flexibility. Figure 6 depicts possible solution conformations of compounds **5** and **6**. Because these conformers are quite similar, one would not expect a large difference in energy penalties incurred in binding to the protein.

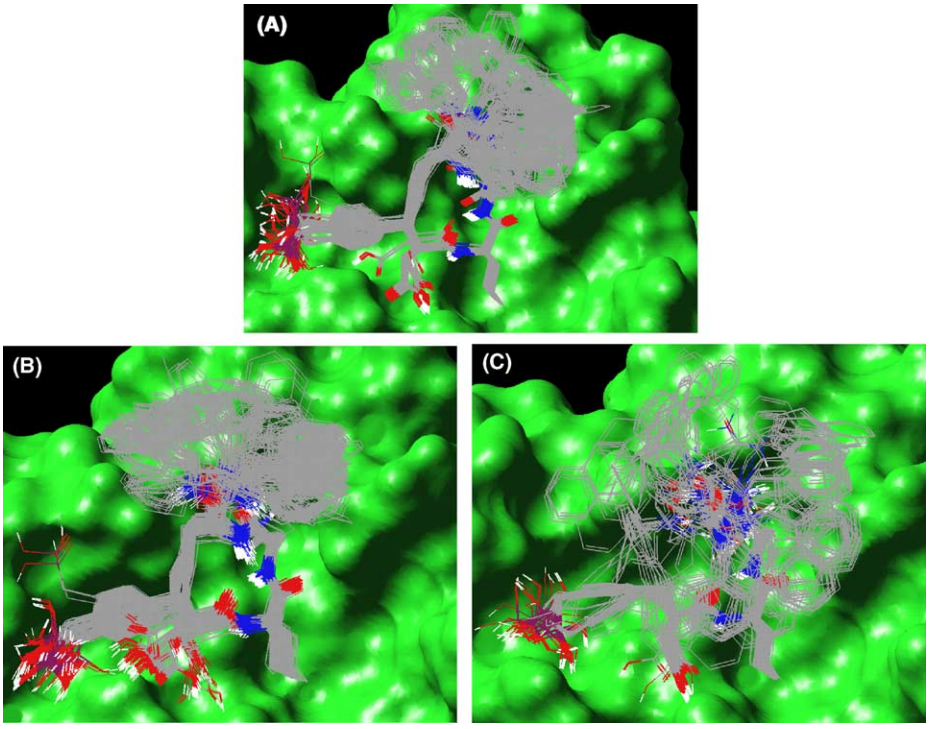

Figure 7. Overview of the probable Grb2 SH2 domain binding modes of **5** (A; 311 conformers); **6** (B; 250 conformers); and **7** (C; 126 conformers) obtained by conformational searches of the compounds within the binding pocket.

The poorer binding affinity of peptide **7** may be attributed to its greater conformational flexibility, which could result in higher entropy losses upon binding. To confirm this, a parallel study was conducted wherein the conformational spaces of ligands bound in the active site were explored. While complexed within the active site, peptides **5**, **6**, and **7** were subjected to 1000 steps of a MCMM conformational search routine while keeping the protein atoms fixed. All conformers that were within 50 kcal/mol of the global minimum were saved and analyzed. It was evident from the ensemble of conformations within the active site, that ligands can bind in several ways (Fig. 7). Critical protein interactions of macrocycles **5** and **6** were highly similar, except for variation in the orientation of their naphthylmethylamide moieties. Therefore, although the predicted binding of **5** in its lowest energy conformation was not as favorable as **6**, the fact that its naphthylmethylamide moiety could make more extensive hydrophobic interactions with the protein provided a basis for its experimentally-observed higher SPR binding affinity. On the other hand **7** does not appear to bind in any predominantly favorable mode. The lower SPR binding affinity of **7** may reflect that conformational flexibility is deleterious to binding.

2. Conclusions

The current study further demonstrates the potential value of RCM macrocyclization for the construction of Grb2 SH2 domain-binding peptide mimetics, wherein the role of macrocyclization is to pre-order solution conformations to those favoring high affinity binding. The focus of this work has been i to i + 3 ring closures using allylglycines and β-vinyl-functionalized residues giving rise to minimal macrocyclic tetrapeptide mimetics. This general approach may be applicable to other systems where small peptides would benefit from conformational restriction to bend geometries.

3. Experimental

3.1. Grb2 SH2 domain protein

Oligonucleotides and plasmids. pDonr223 is a Gateway Donor vector modified from pDonr201 (Invitrogen). pDonr223 replaces the kanamycin resistance gene with a gene encoding spectinomycin resistance, and contains several sequencing primer sites to aid in sequence verification of Entry clones. pDest-566 is a Gateway Destination vector containing a T7 promoter, which produces an aminoterminal His6-MBP (maltose binding protein, New England Biolabs) fusion of any protein cloned into the vector using Gateway recombination. The following oligonucleotides (Operon, Inc) were used in this study:

L718: 5′-ATTTTCGAGGCCCAGAAAATTGAGTGGCACGACGGCTGGTTTTTTGGCAAAATCCCCAG
L722: 5′-GGGGACAACTTTGTACAAGAAAGTTGGCTATATGTCCCGCAGGAATATCTGCTGG
L726: 5′-GGGGACAACTTTGTACAAAAAAGTTGGCGAAAACCTGTACTTCCAAGGCCTGAACGATATTTTCGAGGCCCAGAAAATTG

3.2. Cloning of Grb2 SH2 domain fusion protein

A fragment of the Grb2 domain consisting of amino acids 60–151 inclusive was cloned by PCR from IMAGE cDNA library clone #3345525 (Open Biosystems). The fragment was first amplified for 5 cycles using primers L718 and L722 (above), followed by the addition of the adapter primer L726 and amplification was continued for 15 cycles. PCR was carried out using Platinum Taq HiFidelity (Invitrogen) under standard conditions using a 30 s extension time. The final PCR product contains the Grb2 SH2 domain fragment flanked on the 5′ side with a Gateway attB1 site, Tev protease cleavage site, and a 15 amino acid peptide (BAP), which can be biotinylated in vivo in *E. coli*. The 3′ side contains a Gateway attB2 site. The PCR product was cleaned using the QiaQuick PCR purification kit (Qiagen) and recombined into pDonr223 using the Gateway BP recombination reaction (Invitrogen) with the manufacturer's protocols. The subsequent Entry clone was sequence verified, and sub-cloned by Gateway LR recombination into pDest-566. Final expression clones encode for a protein of the form His6-MBP-B1-tev-BAP-Grb2(60–151)-stop. The linker between the MBP and the Grb2 regions consists of the amino acid sequence ENLYFQGLNDIFEAQKIEWHEG, which is cleaved by Tev protease between the Q and G residues to leave the BAP peptide, which can be biotinylated on the lysine residue.

3.3. Expression of Grb2 SH2 domain fusion protein

The Grb2 SH2 domain expression clone was transformed into *E. coli* BL21(DE3) cells, which also contained the pBirA plasmid (Avidity, Inc) that overexpresses the *E. coli* biotin ligase protein. Cells were grown to mid-log phase in Circlegrow medium (Qbiogene) at 37 °C, shifted to 16 °C, and induced by adding 0.5 mM biotin and 0.5 mM IPTG. Growth was continued for 18 h and cells were harvested by centrifugation. Pellets were frozen at −80 °C prior to subsequent processing.

3.4. Purification of the His_6-MBP:Grb2 fusion protein and Grb2 SH2 domain protein

The cell paste from 6 L of an *E. coli* expression culture was resuspended with two volumes of extraction buffer (20 mM Na phosphate, pH 7.5, 100 mM NaCl, 1 mM bME, 5% glycerol, 20 mM imidazole, and complete protease inhibitor (Roche) at 1 tablet per 50 mL of extraction buffer) per gram wet weight of cells, digested with lysozyme (0.5 mg/mL) for 30 min on ice, adjusted to 5 mM $MgCl_2$ and treated with 10 U benzonase (Novagen)/mL for an additional 20 min. The sample was sonicated to lyse the cells (verified by microscopic examination), adjusted to 500 mM NaCl, clarified by centrifugation (27,000*g* for 30 min) and filtration (0.45 μm, PES membrane) and applied at 1.0 mL/min

to a 5 mL chelating sepharose column (Amersham) previously charged with nickel and equilibrated with extraction buffer in 500 mM NaCl (binding buffer). The column was washed with binding buffer to baseline and proteins were eluted over a 100 mL gradient to 400 mM imidazole at 2 mL/min, collected in 2 mL fractions and analyzed by SDS-PAGE.

Fractions from the immobilized metal ion affinity chromatography (IMAC) that contained the His_6-MBP:Grb2 SH2 domain fusion protein were pooled and then divided: 20% was dialyzed against 25 mM HEPES, pH 7.4, and 80% was dialyzed against binding buffer without imidazole. Samples of the latter fraction were titrated with TEV protease. The TEV protease digestions were scaled up based on the results of the test digests. Final Grb2 SH2 domain purification was performed as an additional IMAC step similar to the initial IMAC save for the absence of imidazole in the sample and the separation of the gradient into two sections. The first gradient was over 50 mL from 0–50 mM imidazole, while the second gradient was over 50 mL from 50–400 mM imidazole. Final protein pools were dialyzed against $1 \times$ PBS, pH 7.2, and concentrated to 1 mg/mL using Amicon Ultra concentrators (Millipore).

3.5. HPLC purification and characterization of recombinant Grb2 SH2 domain protein

The Grb2 SH2 domain protein was purified on a nickel column and digested with TEV protease as described above. After digestion the protein was subjected to chromatography on a second nickel column to eliminate released MBP and TEV protease. For further purification the protein was subjected to reverse phase HPLC on a C_{18} column Delta-Pak (25×100 mm, 15 μm; Waters, Milford, MA). In a typical fractionation, 100 μL of TFA was added to 25 mL of protein solution and this was injected on the column equilibrated in buffer A (0.1% aqueous TFA). Proteins were eluted using a linear gradient of buffer B (0.1% TFA in acetonitrile) from 0% to 90% over 60 min with a flow rate of 7 mL/min using UV detection at 254 nm. One major peak was collected, which upon MALDI-TOF mass spectrometric analysis revealed the presence of a protein with mass of 12784 Da. This is in agreement with the theoretical mass of the desired biotinylated protein (12562 + 226 = 12788 Da). The corresponding fractions from seven injections were combined to give a total volume of 52 mL. A 2 μL aliquot of the combined material was analyzed using N-terminal protein sequencing. The resulting 19 amino acid sequence 'GLNDIFEAQXIEWHDGWFF' was in agreement with the expected sequence. The PTH derivative of the residue in position 10 eluted between arginine and tyrosine, corresponding to the biotinylated lysine. No residual non-modified lysine was detected at this stage, indicating quantitative biotinylation. The results of amino acid analysis of the preparation were consistent with the expected amino acid composition of the protein and indicated a protein content of 28 μg per 100 μL. The preparation was lyophilized in 2.1 mg aliquots based on the results of amino acid analysis.

3.6. Biosensor analysis

Binding experiments were performed on Biacore S51 instrument (Biacore Inc., Piscataway NJ). All biotinylated Grb2 SH2 domain proteins (b-Grb2) were expressed and purified as described above. The b-Grb2 was immobilized onto carboxymethyl 5′ dextran surface (CM5 sensor chip, Biacore Inc.) by amine coupling. The lyophilized b-Grb2 was reconstituted in 50% aqueous DMSO to make a stock solution of 1 mg/mL and stored at −80 °C. A 1:12.5 dilution of b-Grb2 was used for immobilization, following dilution in acetate buffer pH 5.0 and using 5% DMSO. 1XPBS (phosphate buffered saline, pH 7.4) as the running buffer.

An immobilization wizard was used to aim for the immobilization target. Approximately 2500–5000 resonance units (RU) of b-Grb2 protein were captured onto the CM5 sensor chip. Synthetic peptides **5**, **6** and **7** were serially diluted in running buffer to the concentrations (1.25–1500 nM) as described in each sensorgram and injected at 25 °C at a flow rate of 30 mL/min for 2 min. Samples containing different concentrations of peptides were injected in increasing concentration, and every injection was performed in duplicate within each experiment. In order to subtract background noise from each data set, all samples were also run over an unmodified reference surface and random injections of running buffer were performed throughout every experiment ('double referencing'). Data were fit to a simple 1:1 interaction model, using the global data analysis program CLAMP.[30]

3.7. NMR solution studies

NMR data were collected on a Varian Unity Inova instrument operating at 500 MHz. All NMR data were collected at 25 °C. Assignments were made using standard NMR experiments. In 100% D_2O, 1D ^1H NMR data were collected using pre-saturation for the residual H_2O and standard 2D NMR experiments were conducted, including NOESY (at mix times of 50 and 200 ms), dqCOSY, and TOCSY. 1D ^1H NMR data were collected in 10% D_2O (90% H_2O) using Watergate suppression and standard wgNOESY, wgROESY, and wgTOCSY 2D experiments were run. Samples were prepared as follows: A total of 1.79 mg of **7** as a lyophilized solid in free acid form was dissolved in 600 μL H_2O/D_2O (pH 3.29) and a total of 0.53 mg of **5** as a lyophilized solid in free acid form was dissolved in 600 μL H_2O/D_2O (pH 5.04). Peptide **6** was insoluble in water in the free acid form. Therefore, a total of 2.245 mg of **6** in its sodium salt form was dissolved in 600 μL H_2O/D_2O (pH 7.9). Potential intramolecular hydrogen bonding interactions were investigated by measuring the exchange rates for the exchangeable protons of the N–H groups. This was achieved by taking the samples up in 200 mL of H_2O, followed by lyophilization to dryness (repeated at least 3 times). Immediately prior to NMR measurements, samples were taken up in 100% D_2O. The 1D ^1H NMR experiments were monitored over a time course from 5 min to 24 h. Protons were integrated over the same region for each spectrum and referenced to a non-exchangeable proton with an integration value

of 1. Integration decreased as each N–H proton underwent deuterium exchange. The integral of each exchangeable proton was plotted as a function of time and fit to the following equation:

$$y = y_0 + A * \exp(R_0 * x),$$

where y = integrated area and x = time (min)

For **6** in its sodium salt form, complete exchange was observed within 5 min, rendering it impossible to derive relative exchange rates.

3.8. Molecular modeling

All simulations were performed using the molecular modeling tools available within Macromodel 8.0.[31] Chain A from the crystal structure of mAZ–pY–(αMe)-pY–N–NH_2 bound to the Grb2 SH2 domain (1JYQ.pdb[32]) was used as the starting geometry for the modeling study. All crystallographic water molecules were removed and the structure of the bound ligand was modified using the 3D-sketcher tools available within Macromodel 8.0 to yield initial structures of peptides **5**, **6**, and **7** complexed with the protein. Each of the resulting protein–ligand complexes was then subjected to minimization using the Polak-Ribier Conjugate gradient (PR-CG) method until a gradient convergence threshold of 0.05 was reached. This was followed by 10 ps of equilibration and 50 ps of molecular dynamics simulation using the Merck Molecular Force Field (MMFFs)[27] and a continuum solvation model for H_2O (GB/SA).[28] For each compound under study, 100 structures of the protein–ligand complex from molecular dynamics simulations were saved for further analysis. The frames with the lowest energy of the 100 saved structures are depicted in Figure 5. During minimization and simulation, all atoms were held fixed except for those within a 10 Å sphere around the ligands. In an attempt to explore the conformational flexibility of the molecules while bound to the protein, the lowest energy frames of peptides **5**, **6**, and **7** complexed with the Grb2 SH2 domain were subjected to 1000 steps of Monte Carlo Multiple Minimum (MCMM)[26] conformational search routine while keeping the protein atoms fixed. In a separate study, the structures of **5**, **6**, and **7** were extracted out from their complexed state and subjected to 5000 steps of MCMM using MMFFs with a continuum solvation model for H_2O. All conformers within 50 kcal/mol of the global energy minimum were saved and subjected to cluster analysis using XCluster.[29] Conformations of the molecules that formed clusters with high separation ratios were saved and the inter-proton distances were measured using the analysis tool in Macromodel 8.0. These distances were compared with the inter-proton distances obtained from NMR NOESY data to derive the possible solution conformers.

References and notes

1. Lowenstein, E. J.; Daly, R. J.; Batzer, A. G.; Li, W.; Margolis, B.; Lammers, R.; Ullrich, A.; Skolnik, E. Y.; Barsagi, D.; Schlessinger, J. *Cell* **1992**, *70*, 431–442.
2. Buday, L.; Downward, J. *Cell* **1993**, *73*, 611–620.
3. Janes, P. W.; Daly, R. J.; deFazio, A.; Sutherland, R. L. *Oncogene* **1994**, *9*, 3601–3608.
4. Dankort, D.; Maslikowski, B.; Warner, N.; Kanno, N.; Kim, H.; Wang, Z. X.; Moran, M. F.; Oshima, R. G.; Cardiff, R. D.; Muller, W. J. *Mol. Cell. Biol.* **2001**, *21*, 1540–1551.
5. Fretz, H.; Furet, P.; Garcia-Echeverria, C.; Rahuel, J.; Schoepfer, J. *Curr. Pharm. Des.* **2000**, *6*, 1777–1796.
6. Garcia-Echeverria, C. *Curr. Med. Chem.* **2001**, *8*, 1589–1604.
7. Kessels, H. W. H. G.; Ward, A. C.; Schumacher, T. N. M. *Proc. Natl. Acad. Sci. U.S.A.* **2002**, *99*, 8524–8529.
8. Rahuel, J.; Gay, B.; Erdmann, D.; Strauss, A.; Garcia-Echeverria, C.; Furet, P.; Caravatti, G.; Fretz, H.; Schoepfer, J.; Grutter, M. G. *Nat. Struct. Biol.* **1996**, *3*, 586–589.
9. Gay, B.; Furet, P.; Garcia-Echeverria, C.; Rahuel, J.; Chene, P.; Fretz, H. *Biochem* **1997**, *36*, 5712–5718.
10. Ettmayer, P.; France, D.; Gounarides, J.; Jarosinski, M.; Martin, M. S.; Rondeau, J. M.; Sabio, M.; Topiol, S.; Weidmann, B.; Zurini, M.; Bair, K. W. *J. Med. Chem.* **1999**, *42*, 971–980.
11. Miller, S. J.; Blackwell, H. E.; Grubbs, R. H. *J. Am. Chem. Soc.* **1996**, *118*, 9606–9614.
12. Gao, Y.; Voigt, J.; Wu, J. X.; Yang, D.; Burke, T. R., Jr. *Bioorg. Med. Chem. Lett.* **2001**, *11*, 1889–1892.
13. Wei, C.-Q.; Gao, Y.; Lee, K.; Guo, R.; Li, B.; Zhang, M.; Yang, D.; Burke, T. R., Jr. *J. Med. Chem.* **2003**, *46*, 244–254.
14. Shi, Z.-D.; Wei, C.-Q.; Lee, K.; Liu, H.; Zhang, M.; Araki, T.; Roberts, L. R.; Worthy, K. M.; Fisher, R. J.; Neel, B. G.; Kelley, J. A.; Yang, D.; Burke, T. R., Jr. *J. Med. Chem.* **2004**, *47*, 2166–2169.
15. Shi, Z.-D.; Lee, K.; Wei, C.-Q.; Roberts, L. R.; Worthy, K. M.; Fisher, R. J.; Burke, T. R., Jr. *J. Med. Chem.* **2004**, *47*, 788–791.
16. Oishi, S.; Shi, Z.-D.; Worthy, K. M.; Bindu, L. K.; Fisher, R. J.; Burke, T. R., Jr. *ChemBioChem*, in press.
17. Pernerstorfer, J.; Schuster, M.; Blechert, S. *Chem. Commun. (Cambridge)* **1997**, 1949–1950.
18. Hanessian, S.; Angiolini, M. *Chem. Eur. J.* **2002**, *8*, 111–117.
19. Schmiedeberg, N.; Kessler, H. *Org. Lett.* **2002**, *4*, 59–62.
20. Dekker, F. J.; de Mol, N. J.; Fischer, M. J. E.; Kemmink, J.; Liskamp, R. M. J. *Org. Biomol. Chem.* **2003**, *1*, 3297–3303.
21. Plake, H. R.; Sundberg, T. B.; Woodward, A. R.; Martin, S. F. *Tetrahedron Lett.* **2003**, *44*, 1571–1574.
22. Davidson, J. P.; Lubman, O.; Rose, T.; Waksman, G.; Martin, S. F. *J. Am. Chem. Soc.* **2002**, *124*, 205–215.
23. Grunwald, E.; Steel, C. *J. Am. Chem. Soc.* **1995**, *117*, 5687–5692.
24. Rose, G. D.; Gierasch, L. M.; Smith, J. A. *Adv. Protein Chem.* **1985**, *37*, 1–109.
25. Notation as proposed by Eck et al. *Nature* **1993**, *362*, 87–91.
26. Chang, G.; Guida, W. C.; Still, W. C. *J. Am. Chem. Soc.* **1989**, *111*, 4379–4386.
27. Halgren, T. A. *J. Comput. Chem.* **1996**, *17*, 490–519.
28. Qiu, D.; Shenkin, P. S.; Hollinger, F. P.; Still, W. C. *J. Phys. Chem. A* **1997**, 3005–3014.
29. Shenkin, P. S.; McDonald, D. Q. *J. Comput. Chem.* **2004**, *15*, 899–916.
30. Myszka, D. G.; Morton, T. A. *Trends Biochem. Sci.* **1998**, *23*, 149–150.
31. Mohamadi, F.; Richards, N. G. J.; Guida, W. C.; Liskamp, R.; Lipton, M.; Caufield, C.; Chang, G.; Hendrickson, T.; Still, W. C. *J. Comput. Chem.* **1990**, *11*, 440–467.
32. Nioche, P.; Liu, W.-Q.; Broutin, I.; Charbonnier, F.; Latreille, M.-T.; Vidal, M.; Roques, B.; Garbay, C.; Ducruix, A. *J. Mol. Biol.* **2002**, *315*, 1167–1177.